Salt Influences on Natural Hydrocarbon Migration Pathways: Part 1 – Modeling of Near-Salt Stress

Zihao Li[1], Jenny Suckale[1], Leslie Baksmaty[2], Daniel Minisini[2]

1 Department of Geophysics, Stanford University, Stanford, CA 94305, USA
2 Shell International Exploration and Production Inc., Houston, TX 77082, USA

†Corresponding author: XXXXXX@stanford.edu

Abstract
Natural hydrocarbon seepage.

Keywords hydrocarbon migration pathway • salt •

1. Introduction

Natural hydrocarbon seepage is a natural phenomenon in which hydrocarbons escape from the ground, occurring either on land or beneath the ocean above subsurface hydrocarbon sources and accumulations (Kennicutt, 2017). Natural hydrocarbon seepage has been observed globally in locations such as the Adriatic Sea (Rovere et al., 2020), the Aquitaine Shelf (Dupré et al., 2014), the Black Sea (Kruglyakova et al., 2004), the Central Nile Deep Sea Fan (Dupré et al., 2007), the Gulf of Mexico (Bernard et al., 1976), the Makran continental margin (Römer et al., 2012), the Sea of Marmara (Zitter et al., 2008), the North Sea (Borges et al., 2016), the northern shelf of the Santa Barbara Basin (Fischer and Andrew, 1973), the northern US Atlantic Margin (Skarke et al., 2014), and the South China Sea (Feng et al., 2018), among others. Natural hydrocarbon seepage not only has the potential to cause economic losses but also contaminates the marine ecosystem (Leifer, 2019). Hydrocarbons often naturally seep from the seabed in the form of gas, and these gases are mainly composed of methane and form bubbles that rise from the seabed (Bernard et al., 1976; Claypool et al., 1983; Wang et al., 2016). In another scenario, hydrocarbons naturally seep from the seabed in the form of oil and gas mixture (Whelan et al., 2005; Wang et al., 2016). These spilled oils can pollute surrounding waters and pose a threat to marine ecosystems (Bacosa et al., 2022).

Porosity wave is considered a mechanism for hydrocarbon migration from reservoir to seabed (Yarushina et al., 2016; Peshkov et al., 2021; Yarushina et al., 2022). Porosity waves are fluctuations in geological media caused by changes in the internal porosity of rocks (Connolly and Podladchikov, 2012; Connolly and Podladchikov, 1998). The internal porosity of the reservoir is heterogeneous (Figure 1a), and these small differences in heterogeneity can be amplified by the rock matrix deformation and the internal fluid flow, thereby instigating the migration of fluids (Audet and Fowler, 1992; Barcilon & Richter, 1986; Connolly & Podladchikov, 2000; Yarushina et al., 2021). Porosity waves are generally affected by factors such as stress variations, inflow or outflow of fluid in porous media, and chemical reactions (Stevenson, 1989; Richardson, 1998; Omlin et al., 2017; Yarushina et al., 2020). Porosity waves can enable hydrocarbons to form a preferential flow path in a porous medium without fractures, thereby allowing hydrocarbons to migrate from the reservoir to the seabed over extensive timescales (Figure 1b), potentially spanning more than thousands of years (Yarushina et al., 2021). However, field data suggest that the natural hydrocarbon seepage rate predicted by porosity wave model is two to three orders of magnitude less than the actual field seepage rate. Considering that subsurface hydrocarbon migration can occur at rates faster than those predicted by porosity wave models, the study of subsurface hydrocarbon migration pathways is important in the field of natural hydrocarbon seepage research.

Numerous studies have found that hydrocarbons can migrate towards the seabed through faults or fractures (Figure 1c) in the subsurface formations (Hunt, 1995; Whelan, 2005). Seepage primarily occurs in tectonically active regions (Van der Meer et al., 2000). This is because methane can dissolve in migrating pore water, which often migrates and accumulates in the fault zones, resulting in natural seepage (Judd, 2003). The spatial and temporal inhomogeneity of the methane seepage through faults complicates the estimation of actual hydrocarbon fluxes involved (Whelan, 2005). Beyond the influence of fractures and faults on hydrocarbon migration pathways, there may indeed be other mechanisms by which hydrocarbons may not migrate along faults (Geyer and William, 1972; Løseth et al., 2011). However, in the Gulf of Mexico, hydrocarbon flow along faults and fractures is the primary mechanism for natural hydrocarbon seepage (Geyer and William, 1972). The Gulf of Mexico has many salt formations that are associated with numerous near-surface faults and some of the most abundant oil reservoirs (Geyer and William, 1972). Some studies, through well logging data and seismic imaging, indicate that hydrocarbons can seep above salt formations (Figure 1d) (Schroot and Schüttenhelm, 2003; Heggland 2004).

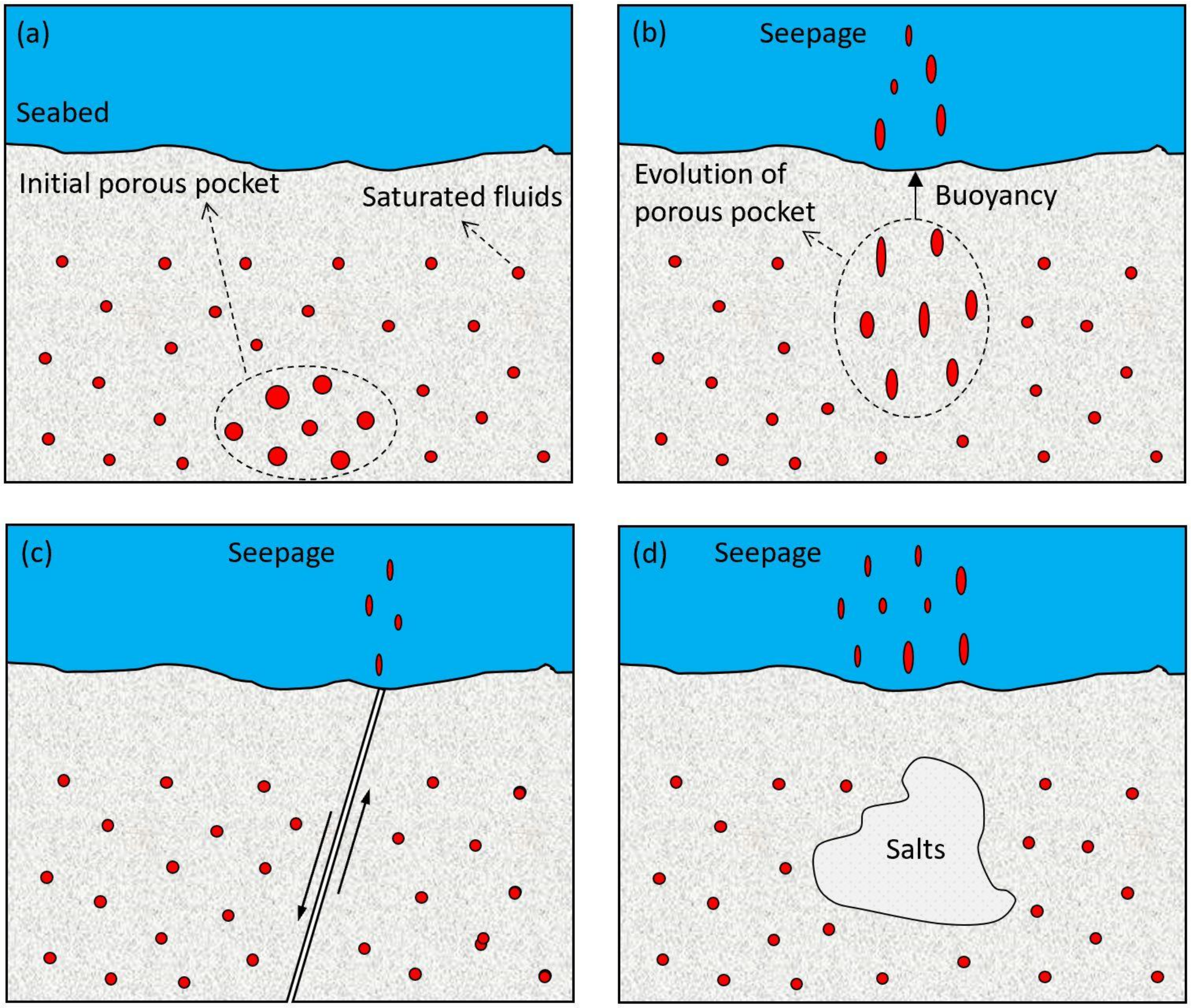

Figure 1. Schematics of natural hydrocarbon seepage summarized from literature. (a) Porosity wave mechanism. The rocks initially have small heterogeneity. (b) Porosity wave mechanism. The porous pocket flows upward over time, creating porosity waves all the way to the seabed. The fluids seep out when it reaches the seabed. (c) Observations related to faults. Fluids seep from fault zones on the seabed in the form of gas bubbles or oil and gas mixtures. (d) Observations related to salt. Natural hydrocarbon seepage often occurs above salt. This is the type often observed in the Gulf of Mexico.

Rock salt, primarily composed of sodium chloride (NaCl), commonly forms in environments such as salt lakes and oceans, resulting from the evaporation of water bodies (Rodriguez-Valera, 2020). Over geological time, rock salt can be deeply buried, and gradually form salt beds or salt domes, which are widely distributed all over the earth (Nettleton, 1934). Salt typically has a larger viscosity than common reservoir rocks such as sandstone (10^{15} – 10^{16} Pa·s) and shale (10^{13} – 10^{14} Pa·s) (Makhnenko and Podladchikov, 2018; Mukherjee et al., 2010). In addition, salt cannot sustain deviatoric stress. Salt deforms through plastic (isovolumetric) creep when the mean stress exceeds approximately 5 MPa (725 psi), and the stress relaxes to an isotropic stress state with equal horizontal and vertical stresses (Fredrich et al., 2003). These unique properties of salt result in complex local stress distributions at the interface between salt and reservoir rocks (Fredrich et al., 2003; Nikolinakou et al., 2014). Variations in hydrostatic pressure and lithospheric stress influence the seepage of hydrocarbons (Awadh et al., 2013). Although salt formations are the most effective seal in a hydrocarbon system, they are not a perfect seal and commercial volumes of hydrocarbons can occasionally migrate through salt over short time scales (Davison, 2009). Salt may lead to shallow hydrocarbons seeping into the seabed through faults above salt (Schroot and Schüttenhelm, 2003; Heggland 2004), while deeper hydrocarbons could potentially penetrate the salt itself. Therefore, assessing the stress distribution around salt formation is critical for interpreting the processes of hydrocarbon migration.

In this paper, we model the stress distribution around salt and evaluate its impact on the pathways of hydrocarbon migration. We first present a numerical model to simulate stress distribution around salt. This model is predicated on Stokes flow; we have rendered the equations dimensionless and solved the numerical model using the pseudo-transient method. Subsequently, the results calculated from this model are validated under a given in-situ stress gradient. The real geometric shape of rock salt is then incorporated into this model, and the stress field of the formation is computed. Finally, we use a fracture criterion that considers hydrocarbon migration to identify potential fracture areas.

2. Model Development

2.1 Mathematical model

Salt is a material characterized by its fluidity, and we model it as an incompressible, nonlinear viscous ~~creep~~ material. The mass balance for an incompressible material can be expressed as,

$$\nabla \cdot \mathbf{v} = 0 \,, \tag{1}$$

where **v** is the velocity of the rock matrix. Because the velocity of the rock matrix is super small, the inertial forces are negligible compared to viscous forces, and the convective acceleration terms in Navier-Stokes equation can be neglected. The primary forces in subsurface formations stem from gravity and tectonic stress, thus the body force term in Stokes equation corresponds to the gravitational force of the material. Therefore, the Stokes equation of the material can be expressed as,

$$-\nabla p + \nabla \cdot \left(\mu(\boldsymbol{\tau}) \left(\nabla \mathbf{v} + (\nabla \mathbf{v})^T \right) \right) + \rho \mathbf{g} = 0 \,, \tag{2}$$

Where p is the isotropic pressure of the rock material, $\boldsymbol{\tau}$ is the deviatoric stress tensor. Given that our rock model is constructed on the basis of a fluid model, we define the compressive stress in the rock matrix as negative and the tensile stress as positive. This notation is contrary to the conventional rock mechanics practice where compressive stress is typically considered positive. Therefore, the Cauchy stress tensor ($\boldsymbol{\sigma}$) is calculated using the deviatoric stress tensor and the isotropic pressure ($\boldsymbol{\sigma} = \boldsymbol{\tau} - p\mathbf{I}$). The variable μ is the rock viscosity, **g** is the gravity and ρ is the rock density. Salt and background rocks have different viscosities and densities. We assume that the rock densities are constant. The density of the salt is 2200 kg/m^3, and the density of the background rock is calculated from the vertical stress gradient.

Figure 2 shows the schematic of a subsurface formation containing salt inclusions. According to our field data, the seabed is situated approximately 800 m below sea level. The upper surface of the formation is subjected to hydrostatic pressure, with an estimated seawater density of 1020 kg/m^3. The gradient of the minimum horizontal stress (γ_h) is quantified as 16.97 kPa/m (0.75 psi/ft), and that of the vertical stress (γ_v) as 19.23 kPa/m (0.85 psi/ft). In the context of the 3D model, the maximum horizontal stress is determined as the mean of the minimum horizontal stress and the vertical stress. In the mathematical model, we use the finite difference method to compute the stress distribution within the subsurface formation. The stress experienced by each element is determined based on the stress gradient,

$$\sigma_{x,element} = \gamma_h \cdot h, \tag{3}$$

$$\sigma_{z,element} = p_w + \gamma_v \cdot h, \tag{4}$$

where p_w is the water pressure at the seabed, h is the depth of the element position. The dimension of this formation is 130 km × 7 km. The parameters of the model need to be nondimensionalized. Given the substantial size of the model, solving 3-D model using Newton's method would significantly increase computational time, and nondimensionalization helps bring the model into a manageable simulation scale. In Section 2.4, we use the pseudo-transient method to solve the nondimensionalized model.

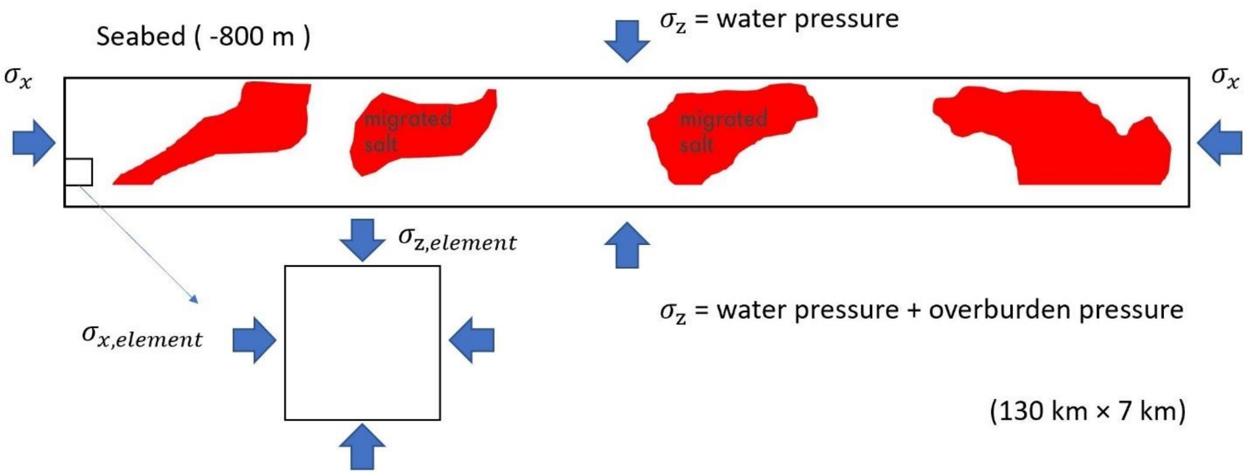

Figure 2. Schematic of a subsurface formation containing salt inclusions (red). The dimension of this formation is 130 km × 7 km. The minimum horizontal stress gradient is 16.97 kPa/m (0.75 psi/ft), and the vertical stress gradient is 19.23 kPa/m (0.85 psi/ft).

2.2 Nondimensionalization

Nondimensionalization, aside from reducing large models to a manageable scale, also helps limit the truncation error of the model. Here we nondimensionalize Equations (1) and (2) in the x-direction, and the same method can be extended to the nondimensionalization of 3D models or any other directions. We introduce a series of scaling factors to calculate the real parameters of the model,

$$x = l_{sc} \cdot \tilde{x},$$

$$p = p_{sc} \cdot \tilde{p},$$

$$\mu = \mu_{sc} \cdot \tilde{\mu},$$

$$\rho = \rho_{sc} \cdot \tilde{\rho},$$

$$\mathbf{v} = v_{sc} \cdot \tilde{\mathbf{v}}, \tag{5}$$

where the subscript '*sc*' denotes the scaling factor, while the superscript '~' indicates a nondimensionalized parameter. We have the nondimensionalized mass balance by substituting Equation (5) into Equation (1),

$$\nabla \cdot \tilde{\mathbf{v}} = 0\,, \tag{6}$$

Using a 2-D model as an illustrative example, we substitute Equation (5) into Equation (2) in the x-direction and z-direction,

$$-\frac{\partial(p_{sc}\tilde{p})}{\partial(l_{sc}\tilde{x})} + \frac{\partial}{\partial(l_{sc}\tilde{x})}\left(2\mu_{sc}\tilde{\mu}\frac{\partial(v_{sc}\tilde{v}_x)}{\partial(l_{sc}\tilde{x})}\right) + \frac{\partial}{\partial(l_{sc}\tilde{z})}\left(\mu_{sc}\tilde{\mu}\left(\frac{\partial(v_{sc}\tilde{v}_x)}{\partial(l_{sc}\tilde{z})} + \frac{\partial(v_{sc}\tilde{v}_z)}{\partial(l_{sc}\tilde{x})}\right)\right) + \rho_{sc}\tilde{\rho}g_x = 0\,,$$

$$-\frac{\partial(p_{sc}\tilde{p})}{\partial(l_{sc}\tilde{z})} + \frac{\partial}{\partial(l_{sc}\tilde{z})}\left(2\mu_{sc}\tilde{\mu}\frac{\partial(v_{sc}\tilde{v}_z)}{\partial(l_{sc}\tilde{z})}\right) + \frac{\partial}{\partial(l_{sc}\tilde{x})}\left(\mu_{sc}\tilde{\mu}\left(\frac{\partial(v_{sc}\tilde{v}_x)}{\partial(l_{sc}\tilde{z})} + \frac{\partial(v_{sc}\tilde{v}_z)}{\partial(l_{sc}\tilde{x})}\right)\right) + \rho_{sc}\tilde{\rho}g_z = 0 \tag{7}$$

Equations (7) need to be simplified such that the coefficients preceding the isotropic pressure and deviatoric stress terms in the Stokes equation remain relatively similar, which can help prevent instability when implementing the pseudo-transient method for solution. By simplifying this equation, we finally have

$$-\frac{\partial\tilde{p}}{\partial\tilde{x}} + \psi\frac{\partial}{\partial\tilde{x}}\left(2\tilde{\mu}\frac{\partial\tilde{v}_x}{\partial\tilde{x}}\right) + \psi\frac{\partial}{\partial\tilde{z}}\left(\tilde{\mu}\left(\frac{\partial\tilde{v}_x}{\partial\tilde{z}} + \frac{\partial\tilde{v}_z}{\partial\tilde{x}}\right)\right) + \psi\tilde{\rho}\frac{g_x}{g} = 0\,,$$

$$-\frac{\partial\tilde{p}}{\partial\tilde{z}} + \psi\frac{\partial}{\partial\tilde{z}}\left(2\tilde{\mu}\frac{\partial\tilde{v}_z}{\partial\tilde{z}}\right) + \psi\frac{\partial}{\partial\tilde{x}}\left(\tilde{\mu}\left(\frac{\partial\tilde{v}_x}{\partial\tilde{z}} + \frac{\partial\tilde{v}_z}{\partial\tilde{x}}\right)\right) + \psi\tilde{\rho}\frac{g_z}{g} = 0\,, \tag{8}$$

in which

$$\psi = \frac{\rho_{sc}^2 g l_{sc}^3}{\mu_{sc}^2}\,,$$

$$p_{sc} = \frac{\mu_{sc}^2}{\rho_{sc} l_{sc}^2}\,,$$

$$v_{sc} = \frac{\rho_{sc} g l_{sc}^2}{\mu_{sc}} \tag{9}$$

The variable ψ denotes the ratio of buoyancy to viscous drag. Three scaling factors, p_{sc}, ρ_{sc} and μ_{sc}, are used to obtain the nondimensionalized equations.

$$\tilde{\nabla} \cdot \tilde{\mathbf{v}} = 0\,,$$

$$-\tilde{\nabla}\tilde{p} + \psi\tilde{\nabla}\left(\tilde{\mu}\left(\tilde{\nabla}\tilde{\mathbf{v}} + \left(\tilde{\nabla}\tilde{\mathbf{v}}\right)^T\right)\right) + \psi\tilde{\rho}\mathbf{g} = 0\,, \tag{10}$$

Equation (10) is the nondimensionalized governing equations, and we solve them to compute the stress distribution around the salt.

2.3 Salt creep behavior

Creep behavior in rock salt, otherwise referred to as salt creep, signifies a gradual, unceasing, and time-reliant deformation activity that transpires when such salt is exposed to persistent stress. This distinctive activity is derived from the inherent crystalline configuration of rock salt, which permits a slow reshaping and deformation under continuous pressure. As time elapses, this causes a 'creeping' motion or a slow displacement of the salt structure. The Multimechanism Deformation (MD) constitutive model is conceived by considering solitary processes such as the dislocation glide, dislocation climb, as well as a thermally induced mechanism, not precisely defined, but with strong experimental evidence (Fredrich et al., 2003). The inelastic strain component in the MD model is given by,

$$\dot{\varepsilon}_{ij} = \frac{\partial \sigma_{eq}^{c}}{\partial \sigma_{ij}} \dot{\varepsilon}_{eq}^{c}, \tag{11}$$

where σ_{eq}^{c} is the power-conjugate equivalent stress and $\dot{\varepsilon}_{eq}^{c}$ is the power-conjugate equivalent strain rate measures for creep. The volume-preserving and pressure-independent inelastic flow results from dislocation creep, which culminates in a corresponding equivalent stress measure for dislocation creep, which is constructed based on the stress difference, as defined by,

$$\sigma_{eq}^{c} = \left|\sigma_1 - \sigma_3\right|, \tag{12}$$

where σ_1 and σ_3 are the maximum and minimum principal stresses. The kinematic equation that signifies the creep rate, denoted as A, attributable to dislocation flow processes, is expressed as follows,

$$\dot{\varepsilon}_{eq}^{c} = F \sum_{i=1}^{3} \dot{\varepsilon}_{si}, \tag{13}$$

where F stands for a function that symbolizes transient creep behavior, and $\dot{\varepsilon}_{si}$ denotes the steady state strain rate for the distinct dislocation flow mechanism i. The methods encompass dislocation climb (i = 1), dislocation glide (i = 3), and an additional one that is not mechanistically identified but is completely characterized experimentally (i = 2). When the mechanism i = 1 or 2, the steady state strain rates are

$$\dot{\varepsilon}_{si} = A_i e^{-Q_i/RT} \left[\frac{\sigma_{eq}^{c}}{G}\right]^{n_i}, \tag{14}$$

and when the mechanism i = 3, the steady state strain rate is

$$\dot{\varepsilon}_{si} = H\left(\sum_{i=1}^{2} B_i e^{-Q_i/RT}\right) \sinh\left[\frac{q\left(\sigma_{eq}^{c} - \sigma_0\right)}{G}\right], \tag{15}$$

where A_i and B_i are constants, Q_i is the activation energy, R is the universal gas constant, T is the absolute temperature, G is the shear modulus, q is the stress constant, n_i is the stress exponent, σ_0 is the stress limit of the dislocation glide mechanism and H is the Heaviside function with

$\sigma_{eq}^{c} - \sigma_0$ as the argument. The transient function that symbolizes transient creep behavior is given by,

$$F = \begin{cases} \exp\left(\Delta\left(1-\frac{\zeta}{\varepsilon_t^*}\right)^2\right) & , \ \zeta < \varepsilon_t^* \\ 1 & , \ \zeta = \varepsilon_t^* \ , \\ \exp\left(-\delta\left(1-\frac{\zeta}{\varepsilon_t^*}\right)^2\right) & , \ \zeta > \varepsilon_t^* \end{cases} \tag{16}$$

where Δ and δ are the work-hardening and recovery parameters, respectively. The variable ζ is the hardening variable and the variable ε_t^* is the transient strain limit, which can be calculated by

$$\dot{\zeta} = \left(F-1\right)\dot{\varepsilon}_s \ , \tag{17}$$

$$\varepsilon_t^* = K_0 e^{cT}\left(\frac{\sigma_{eq}^{c}}{G}\right)^m \ , \tag{18}$$

where $\dot{\zeta}$ is the evolutional rate of the hardening variable. The variables K_0, c, and m are constants. Note that in the current version of code, work-hardening and recovery (Eq. 16 – 18) are not considered, which should be improved in future development.

2.4 Solution strategy

Salt and the surrounding background rocks have different viscosities, often exhibiting a variance of no less than 2 orders of magnitude. Although the material velocity is the same at the interface between materials of differing viscosities, the abrupt shift in viscosity at this interface results in a discontinuity in pressure and stress, colloquially referred to as a 'jump’ (Suckale, et al. 2010). Three prevalent methods for simulating this pressure jump include the regularization (discontinuities in coefficients and singular sources are smeared out on one or more grids), the dimension-un-splitting (discontinuities are depicted sharply using a local Taylor-series expansion in multiple dimensions), and the dimension-splitting techniques (discontinuities sharply based on multiple local Taylor-series in a single dimension) (Chern and Shu, 2007). In this study, we have employed the regularization technique to numerically treat the interface between salt and background rock.

Additionally, we leverage the pseudo-transient method to derive the solution to our model. Application of the pseudo-transient method necessitates careful testing and selection of the most appropriate parameter sizes within the algorithm, with the aim to optimize the speed of convergence. One can refer to the work detailed in Räss et al., 2020 and Räss et al., 2022 for the selection of parameters and the specifics related to solving Stokes equation using the pseudo-transient method. When using the pseudo-transient method to solve Eq. (1) and Eq. (2), it's necessary to manually introduce the pseudo-time term τ, then we obtain,

$$-\tilde{\nabla} \cdot \tilde{\mathbf{v}} = f_p \ , \tag{19}$$

$$-\tilde{\nabla}\tilde{p}+\psi\tilde{\nabla}\cdot\left(\tilde{\mu}\left(\tilde{\nabla}\tilde{\mathbf{v}}+\left(\tilde{\nabla}\tilde{\mathbf{v}}\right)^{T}\right)\right)+\psi\tilde{\rho}\mathbf{g}=f_{\mathbf{v}}, \tag{20}$$

$$\tilde{\nabla}\tilde{\mathbf{v}}+\left(\tilde{\nabla}\tilde{\mathbf{v}}\right)^{T}=\frac{\tilde{\boldsymbol{\tau}}}{2\tilde{\mu}}+f_{\boldsymbol{\tau}}, \tag{21}$$

where the variables f_p, $f_\mathbf{v}$ and $f_{\boldsymbol{\tau}}$ are all pseudo time derivatives that approach 0 when $\tilde{p}$, $\tilde{\mathbf{v}}$ and $\tilde{\boldsymbol{\tau}}$ converge. Eq. (19) – (21) are the modified nondimensionalized mass balance, modified nondimensionalized Stokes equation and modified nondimensionalized deviatoric stress. Owing to the use of the MD constitutive model for calculating the inelastic strain component, it is imperative that we subtract this component accordingly within the pseudo-transient iteration cycle,

$$\boldsymbol{\tau}=\frac{\boldsymbol{\tau}_{old}+2G\Delta t\left(\boldsymbol{\varepsilon}-\boldsymbol{\varepsilon}_{in}\right)}{G\Delta t/\left(\mu+1\right)}, \tag{22}$$

where $\boldsymbol{\tau}_{old}$ represents the deviatoric stress at the previous iteration step, and the calculated deviatoric stress is then nondimensionalized and substituted into Eq. (19) – (21). The pseudo-transient method functions by strategically adding a pseudo-time term to the equation under analysis. This addition essentially acts as a catalyst, facilitating a more rapid convergence to obtain the solution. A comprehensive guide can be found in Räss et al., 2022 on choosing parameters when utilizing the pseudo-transient method to solve this category of Stokes equations.

3. Results

3.1 Benchmark

Validate

3.2 Salt inclusion

Show stress distribution at the interface between circular salt and BG rock.

3.3 Viscous vs. Viscous Creep

Compare

4. Discussion

4.1 Stress distribution around salt in the Gulf of Mexico

Show real stress distribution, compare it with real stress measurement.

4.2 Potential fracture area

Discuss the effects on hydrocarbon migration pathways.

5. Conclusions

Results show that:

- Stress

Compliance with ethical standards

Conflict of interest

The authors declare that they have no conflict of interest.

Availability of data and material

The authors confirm that the data supporting the findings of this study are available.

Code availability

The code supporting the findings of this study is open source.

Acknowledgements

This material is based upon work supported by Shell Oil USA.

References

Audet, D. M., and A. C. Fowler. "A mathematical model for compaction in sedimentary basins." *Geophysical Journal International* 110, no. 3 (1992): 577-590.

Awadh, Salih Muhammad, Kamal Kareem Ali, and Abbas Taha Alazzawi. "Geochemical exploration using surveys of spring water, hydrocarbon and gas seepage, and geobotany for determining the surface extension of Abu-Jir Fault Zone in Iraq: A new way for determining geometrical shapes of computational simulation models." *Journal of Geochemical exploration* 124 (2013): 218-229.

Bacosa, Hernando Pactao, Sheila Mae B. Ancla, Cris Gel Loui A. Arcadio, John Russel A. Dalogdog, Dioniela Mae C. Ellos, Heather Dale A. Hayag, Jiza Gay P. Jarabe et al. "From Surface Water to the Deep Sea: A Review on Factors Affecting the Biodegradation of Spilled Oil in Marine Environment." *Journal of Marine Science and Engineering* 10, no. 3 (2022): 426.

Barcilon, Victor, and Frank M. Richter. "Nonlinear waves in compacting media." *Journal of Fluid Mechanics* 164 (1986): 429-448.

Bernard, Bernie B., James M. Brooks, and William Malcolm Sackett. "Natural gas seepage in the Gulf of Mexico." *Earth and Planetary Science Letters* 31, no. 1 (1976): 48-54.

Borges, Alberto V., Willy Champenois, Nathalie Gypens, Bruno Delille, and Jérôme Harlay. "Massive marine methane emissions from near-shore shallow coastal areas." *Scientific reports* 6, no. 1 (2016): 1-8.

Chern, I-Liang, and Yu-Chen Shu. "A coupling interface method for elliptic interface problems." *Journal of Computational Physics* 225, no. 2 (2007): 2138-2174.

Claypool, George E., and Keith A. Kvenvolden. "Methane and other hydrocarbon gases in marine sediment." *Annual Review of Earth and Planetary Sciences* 11, no. 1 (1983): 299-327.

Connolly, J. A. D., and Yu Yu Podladchikov. "Compaction-driven fluid flow in viscoelastic rock." *Geodinamica Acta* 11, no. 2-3 (1998): 55-84.

Connolly, J. A. D., and Yu Yu Podladchikov. "Temperature-dependent viscoelastic compaction and compartmentalization in sedimentary basins." *Tectonophysics* 324, no. 3 (2000): 137-168.

Connolly, James AD, and Yury Y. Podladchikov. "An analytical solution for solitary porosity waves: dynamic permeability and fluidization of nonlinear viscous and viscoplastic rock." *Crustal permeability* (2012): 285-306.

Davison, Ian. "Faulting and fluid flow through salt." *Journal of the Geological Society* 166, no. 2 (2009): 205-216.

Dupré, Stéphanie, John Woodside, Jean-Paul Foucher, Gert De Lange, Jean Mascle, Antje Boetius, Vincent Mastalerz et al. "Seafloor geological studies above active gas chimneys off Egypt (Central Nile Deep Sea Fan)." *Deep Sea Research Part I: Oceanographic Research Papers* 54, no. 7 (2007): 1146-1172.

Dupré, Stéphanie, Laurent Berger, Naig Le Bouffant, Carla Scalabrin, and Jean-François Bourillet. "Fluid emissions at the Aquitaine Shelf (Bay of Biscay, France): A biogenic origin or the expression of hydrocarbon leakage?." *Continental shelf research* 88 (2014): 24-33.

Feng, Dong, Jian-Wen Qiu, Yu Hu, Jörn Peckmann, Hongxiang Guan, Hongpeng Tong, Chong Chen et al. "Cold seep systems in the South China Sea: An overview." *Journal of Asian Earth Sciences* 168 (2018): 3-16.

Fischer, Peter J., and Andrew J. Stevenson. "Natural hydrocarbon seeps along the northern shelf of the Santa Barbara Basin, California." In *Offshore Technology Conference*. OnePetro, 1973.

Fredrich, Joanne T., David Coblentz, Arlo F. Fossum, and B. Joe Thorne. "Stress perturbations adjacent to salt bodies in the deepwater Gulf of Mexico." In *SPE annual technical conference and exhibition*. OnePetro, 2003.

Geyer, Richard A., and William E. Sweet. "Natural hydrocarbon seepage in the Gulf of Mexico." In *SPE Symposium on Environmental Conservation*. OnePetro, 1972.

Heggland, Roar. "Hydrocarbon migration and accumulation above salt domes—Risking of prospects by the use of gas chimneys." (2004).

Hunt, J. M. "Petroleum geochemistry and geology (textbook)." *Petroleum Geochemistry and Geology (Textbook).(2 nd Ed.), WH Freeman Company* (1995).

Kennicutt, Mahlon C. "Oil and gas seeps in the Gulf of Mexico." *Habitats and biota of the Gulf of Mexico: Before the deepwater horizon oil spill: Volume 1: Water quality, sediments, sediment contaminants, oil and gas seeps, coastal habitats, offshore plankton and benthos, and shellfish* (2017): 275-358.

Kruglyakova, R. P., Y. A. Byakov, M. V. Kruglyakova, L. A. Chalenko, and N. T. Shevtsova. "Natural oil and gas seeps on the Black Sea floor." *Geo-Marine Letters* 24, no. 3 (2004): 150-162.

Leifer, Ira. "A synthesis review of emissions and fates for the Coal Oil Point marine hydrocarbon seep field and California marine seepage." *Geofluids* 2019 (2019): 1-48.

Løseth, Helge, Lars Wensaas, Børge Arntsen, Nils-Martin Hanken, Christophe Basire, and Knut Graue. "1000 m long gas blow-out pipes." *Marine and Petroleum Geology* 28, no. 5 (2011): 1047-1060.

Judd, Alan G. "The global importance and context of methane escape from the seabed." *Geo-Marine Letters* 23 (2003): 147-154.

Makhnenko, Roman Y., and Yury Y. Podladchikov. "Experimental poroviscoelasticity of common sedimentary rocks." *Journal of Geophysical Research: Solid Earth* 123, no. 9 (2018): 7586-7603.

Mukherjee, Soumyajit, Christopher J. Talbot, and Hemin A. Koyi. "Viscosity estimates of salt in the Hormuz and Namakdan salt diapirs, Persian Gulf." *Geological Magazine* 147, no. 4 (2010): 497-507.

Nettleton, Lewis Lomax. "Fluid mechanics of salt domes." *AAPG Bulletin* 18, no. 9 (1934): 1175-1204.

Nikolinakou, Maria A., Michael R. Hudec, and Peter B. Flemings. "Comparison of evolutionary and static modeling of stresses around a salt diapir." *Marine and Petroleum Geology* 57 (2014): 537-545.

Omlin, Samuel, Benjamin Malvoisin, and Yury Y. Podladchikov. "Pore fluid extraction by reactive solitary waves in 3-D." *Geophysical Research Letters* 44, no. 18 (2017): 9267-9275.

Peshkov, Georgy A., Lyudmila A. Khakimova, Elena V. Grishko, Magnus Wangen, and Viktoria M. Yarushina. "Coupled basin and hydro-mechanical modeling of gas chimney formation: The SW Barents Sea." *Energies* 14, no. 19 (2021): 6345.

Räss, L., Licul, A., Herman, F., Podladchikov, Y. Y., & Suckale, J. (2020). Modelling thermomechanical ice deformation using an implicit pseudo-transient method (FastICE v1. 0) based on graphical processing units (GPUs). Geoscientific Model Development, 13(3), 955-976.

Räss, L., Utkin, I., Duretz, T., Omlin, S., & Podladchikov, Y. Y. (2022). Assessing the robustness and scalability of the accelerated pseudo-transient method. Geoscientific Model Development, 15(14), 5757-5786.

Richardson, Chris N. "Melt flow in a variable viscosity matrix." *Geophysical Research Letters* 25, no. 7 (1998): 1099-1102.

Rodriguez-Valera, Francisco. "Introduction to saline environments." In *The biology of halophilic bacteria*, pp. 1-23. CRC Press, 2020.).

Römer, Miriam, Heiko Sahling, Thomas Pape, Gerhard Bohrmann, and Volkhard Spieß. "Quantification of gas bubble emissions from submarine hydrocarbon seeps at the Makran continental margin (offshore Pakistan)." *Journal of Geophysical Research: Oceans* 117, no. C10 (2012).

Rovere, Marzia, Alessandra Mercorella, Emanuela Frapiccini, Valerio Funari, Federico Spagnoli, Claudio Pellegrini, Andree Soledad Bonetti et al. "Geochemical and geophysical monitoring of hydrocarbon seepage in the Adriatic Sea." *Sensors* 20, no. 5 (2020): 1504.

Schroot, B. M., and R. T. E. Schüttenhelm. "Expressions of shallow gas in the Netherlands North Sea." *Netherlands Journal of Geosciences* 82, no. 1 (2003): 91-105.

Skarke, Adam, Carolyn Ruppel, M. Kodis, D. Brothers, and E. Lobecker. "Widespread methane leakage from the sea floor on the northern US Atlantic margin." *Nature Geoscience* 7, no. 9 (2014): 657-661.

Stevenson, David J. "Spontaneous small-scale melt segregation in partial melts undergoing deformation." *Geophysical Research Letters* 16, no. 9 (1989): 1067-1070.

Suckale, Jenny, Jean-Christophe Nave, and Bradford H. Hager. "It takes three to tango: 1. Simulating buoyancy-driven flow in the presence of large viscosity contrasts." *Journal of Geophysical Research: Solid Earth* 115, no. B7 (2010).

Yarushina, V., L. Räss, and Y. Y. Podladchikov. "Geomechanical origin of focused fluid flow and chimney structures." In *78th EAGE Conference and Exhibition 2016*, vol. 2016, no. 1, pp. 1-5. EAGE Publications BV, 2016.

Yarushina, Viktoriya M., Y. Y. Podladchikov, and L. H. Wang. "Model for (de) compaction and porosity waves in porous rocks under shear stresses." *Journal of Geophysical Research: Solid Earth* 125, no. 8 (2020): e2020JB019683.

Yarushina, Viktoriya M., Roman Y. Makhnenko, Yuri Y. Podladchikov, L. Hongliang Wang, and Ludovic Räss. "Viscous Behavior of Clay-Rich Rocks and Its Role in Focused Fluid Flow." *Geochemistry, Geophysics, Geosystems* 22, no. 10 (2021): e2021GC009949.

Yarushina, Viktoriya M., Lawrence Hongliang Wang, David Connolly, Gábor Kocsis, Ingrid Fæstø, Stephane Polteau, and Assia Lakhlifi. "Focused fluid-flow structures potentially caused by solitary porosity waves." *Geology* 50, no. 2 (2022): 179-183.

Van der Meer, Freek, Paul Van Dijk, Salle Kroonenberg, Yang Hong, and Harold Lang. "Hyperspectral hydrocarbon microseepage detection and monitoring: potentials and limitations." In *Second EARSEl workshop on imaging spectroscopy*, pp. 1-9. 2000.

Wang, Binbin, Scott A. Socolofsky, John A. Breier, and Jeffrey S. Seewald. "Observations of bubbles in natural seep flares at MC 118 and GC 600 using in situ quantitative imaging." *Journal of Geophysical Research: Oceans* 121, no. 4 (2016): 2203-2230.

Whelan, Jean, Lorraine Eglinton, Lawrence Cathles III, Steven Losh, and Harry Roberts. "Surface and subsurface manifestations of gas movement through a N–S transect of the Gulf of Mexico." *Marine and Petroleum Geology* 22, no. 4 (2005): 479-497.

Zitter, Tiphaine AC, Pierre Henry, Giovanni Aloisi, Gilles Delaygue, M. N. Çagatay, B. Mercier De Lepinay, Muna Al-Samir et al. "Cold seeps along the main Marmara Fault in the Sea of Marmara (Turkey)." *Deep Sea Research Part I: Oceanographic Research Papers* 55, no. 4 (2008): 552-570.